JOURNAL OF MATERIALS SCIENCE 22 (1987) 2515–2520

On the formation of stacking faults in silicon implanted with high doses of oxygen

PH. KOMNINOU, TH. KARAKOSTAS, J. STOEMENOS
Physics Department, Aristotle University, 54006 Thessaloniki, Greece
C. JAUSSAUD, J. MARGAIL
Laboratoire d'Etudes de Technologie de l'Informatique, CEN, 38041 Grenoble, France

The stacking faults (SFs) in the silicon overlayer, which is formed after the implantation of silicon wafers by high doses ($2 \times 10^{18}\,cm^{-2}$) of oxygen ions, are studied. During the implantation, a three-dimensional network of SiO_2 precipitates is formed along the $\langle 1\,0\,0 \rangle$ directions. Stacking faults appear only after a high-temperature annealing when all the SiO_2 precipitates are dissolved. Due to the very low value of the anomalous absorption coefficients of silicon, α-fringe contrast profile calculations are needed for the characterization of SFs. The results show that these SFs are extrinsic in character, bounded by Frank partial dislocations.

1. Introduction

The behaviour of oxygen in silicon has been a subject of great interest over recent years, because of its harmful effect in the field of silicon microelectronic circuits, since it induces precipitates and stacking faults during the thermal treatment of the devices [1–3].

In this paper we present transmission electron microscopy (TEM) and cross-sectional electron microscopy (XTEM) observations concerning the formation of stacking faults (SFs) in specimens implanted with high doses of oxygen (SIMOX: an acronym for separation by implanted oxygen) [4].

In the SIMOX technique an SiO_2 buried layer is formed well below the silicon surface by a high dose of oxygen atoms ($\sim 10^{8} O^{+}\,cm^{-2}$) implanted at a fairly high energy ($\sim 200\,keV$). The silicon wafer is heated at about 500° C during the implantation, so that part of the damage produced is cured, preventing the amorphization of the silicon overlayer. The oxygen concentration saturates to form a stoichiometric amorphous buried oxide layer, below the superficial silicon layer, to a depth that depends on the ion energy (for 200 eV at 500 nm). Secondary ion mass spectroscopy [5] and X-ray photoelectron spectroscopy [6] have shown that the oxygen concentration gradually increases from near zero at the surface to a stoichiometric SiO_2 concentration in the buried layer. Although the oxygen concentrations in the wings of the profile are below that of stoichiometric silica, they are still far in excess of the solid solubility levels, resulting in the formation of the SiO_2 precipitates.

By annealing at high temperatures, these precipitates become unstable. A post-annealing at 1300° C dissolves the precipitates, due to the kinetic processes [7], resulting in a silicon overlayer denuded of SiO_2 precipitates. The oxygen migrates to the $Si–SiO_2$ buried layer interface, thus extending the buried layer by 15 to 20% and forming a very sharp $Si–SiO_2$ interface. Such a technology has been developed for fabrication of silicon-on-insulator (SOI) devices and consequently it would be of interest to study the SF formation in these structures. Also, due to the high doses of oxygen implantation, it would be interesting to study the oxygen kinetics and the related phenomena under high oxygen concentrations.

2. Experimental techniques

Oxygen ions were implanted into (1 0 0) device-quality silicon wafers at doses ranging from 1.6×10^{18} to $2.3 \times 10^{18} O^{+}\,cm^{-2}$ at an energy of 200 keV. A specially designed heating stage [8] maintains the temperature of the sample at 600° C, independently of the beam current. The as-implanted specimens were annealed at 1350° C in a nitrogen atmosphere for 6 h. All the specimens were covered by a 0.5 μm protective SiO_2 cupping layer. Specimens for XTEM observations were prepared by the method described by Dupuy [9]. Also, specimens suitable for the plane view of the implanted silicon overlayer were prepared by peeling off this layer from the silicon substrate, dissolving the SiO_2 buried layer with HF. Thus, large implanted areas ($5\,mm^2$) were available for examination. The two methods, TEM and XTEM, are complementary allowing us to have an overall view of the silicon overlayer. A JEM 120CX electron microscope was used for the observations.

3. Results and discussion

The main defects that appear in the as-implanted silicon overlayer are small SiO_2 precipitates, segments of dislocations, small dislocation loops, and large interstitial Frank dipoles sited on the $\{1\,1\,1\}$ planes and localized near the $Si–SiO_2$ buried layer interface. Fig. 1 illustrates the SIMOX structure of an as-implanted specimen. One may observe the silicon overlayer (denoted by AD), the SiO_2 buried layer (DE) and the silicon substrate. In the silicon overlayer there are three distinct zones, the near-surface zone (AB)

0022–2461/87 $03.00 + .12

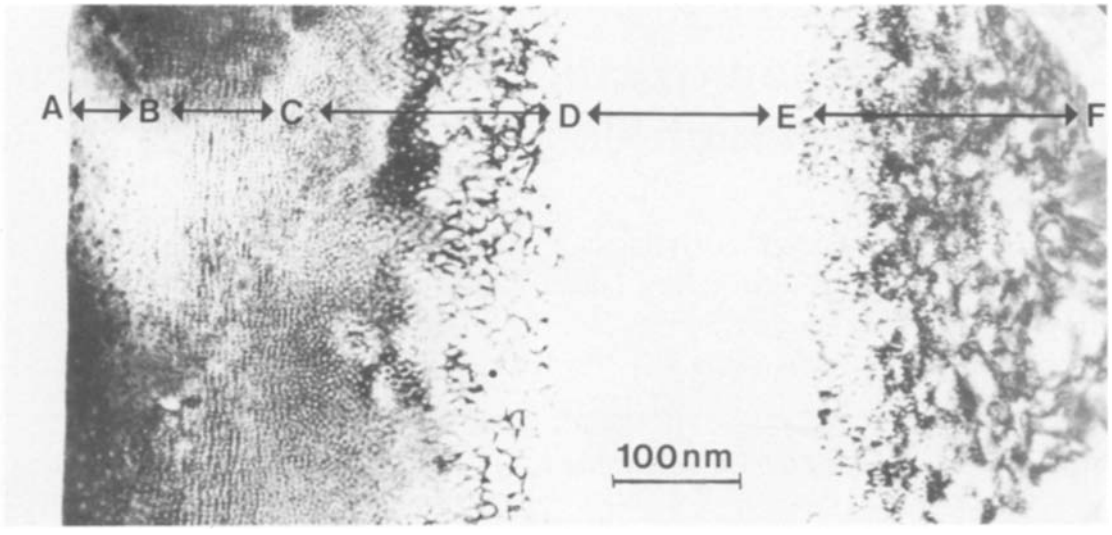

Figure 1 Cross-section of an as-implanted specimen with a dose of $1.5 \times 10^{18} O^+ cm^{-2}$ at 200 keV.

free of precipitates, the intermediate zone (BC) with small SiO_2 precipitates arranged in a periodic manner along the [0 0 1] direction [10–12] and finally the zone (CD), near the Si–SiO_2 interface, where the precipitates are larger, exhibiting a non-uniform columnar or cellular structure. In the silicon substrate there is a zone (EF) near the SiO_2 buried layer which exhibits extended defects such as segments of dislocations, dislocation loops and SiO_2 precipitates; the latter do not form a rippled network as is observed in the BC zone.

The above microstructure was studied in an implanted specimen with a dose of $2.3 \times 10^{18} O^+ cm^{-2}$ at an energy of 200 keV by XTEM and TEM observations. Fig. 2a is a high magnification plane view, (0 0 1) section, of the silicon overlayer which was peeled off from the substrate. The SiO_2 precipitates appear as small dots exhibiting a two-dimensional, almost periodic arrangement. This ordering along the $\langle 1\,0\,0 \rangle$ directions is clearly visible in some areas of the specimen (e.g. A, B, C) in Fig. 2a. There is a misorientation of the precipitates in the areas D, E, F and there is a complete loss of ordering in areas G and H, where the precipitates are arranged randomly. The last applies to areas where the periodic arrangement is disrupted by dislocations [12] or due to the buckling of the film. A diffraction pattern from the same area, which gives integrated information concerning the periodicity of the precipitates, is presented in Fig. 2b. Satellite spots are observed near the main silicon reflections, due to the size effect. Four satellite spots oriented along the [1 0 0] and [0 1 0] directions appear around every main reflection including the origin. However, instead of being sharp their intensity is distributed into small arcs, due to the imperfections of the ordering. From this, we deduce that the misorientation is approximately $\pm 15°$ from the $\langle 1\,0\,0 \rangle$.

To complete the study of the distribution of these precipitates, we performed observations by cross-sectioning the same sample at a (1 1 0) section (Fig. 2c). In the upper part of the silicon overlayer a rippled structure is evident, due to the ordering of the precipitates along the [0 0 1] direction. Along the [1 1 0] direction, the distance between the precipitates is smaller so that they are not well resolved, since they are projected at 45°. Diffraction patterns from the (1 1 0) section also contain satellite spots along the [0 0 1] and [1 1 0] directions (Fig. 2d).

The structure and the morphology of the precipitates has been examined by high resolution observations (see inset in Fig. 2c). The precipitates are amorphous with the smallest having a radius of approximately 1 nm. The silicon matrix surrounding the precipitates is free of strain, as is deduced from the $\{1\,1\,1\}$ lattice image. The $\{1\,1\,1\}$ planes are seen to stop at or pass near the precipitates without any noticeable distortion.

From all these observations we may conclude that the SiO_2 precipitates in the zone CD of Fig. 1 form a three-dimensional network, along the $\langle 1\,0\,0 \rangle$ directions. This arrangement is distorted by the presence of dislocations which, for an as-implanted specimen, have a density of the order of $10^{10} cm^{-2}$. The average spacing of the precipitates in this ordered arrangement is 4.4 nm. The ordered arrangement of the precipitates appears only in the silicon overlayer and not in the substrate, although in the latter the density of the oxide precipitates is as high. This difference in the arrangement is probably related to the mechanism of the silicon self-interstitial migration to the surface [12].

After the annealing at 1350° C for 6 h in a nitrogen atmosphere, all the SiO_2 precipitates were dissolved and most of the oxygen was transferred into the SiO_2 buried layer, extending it by approximately 12% (Fig. 3); the mechanism of the oxygen migration towards the SiO_2 buried layer has been discussed elsewhere [7, 13, 14].

For the as-annealed specimens, the dislocation density was reduced by more than one order of magnitude; however, some stacking faults appeared. Their density was $4 \times 10^5 mm^{-3}$, and their mean length was 0.7 μm with the maximum being approximately 1.5 μm. The SFs lie in all the $\{1\,1\,1\}$ planes (Fig. 4) and they intersect both sides of the silicon overlayer, which in this case has a thickness of 200 nm. This means that

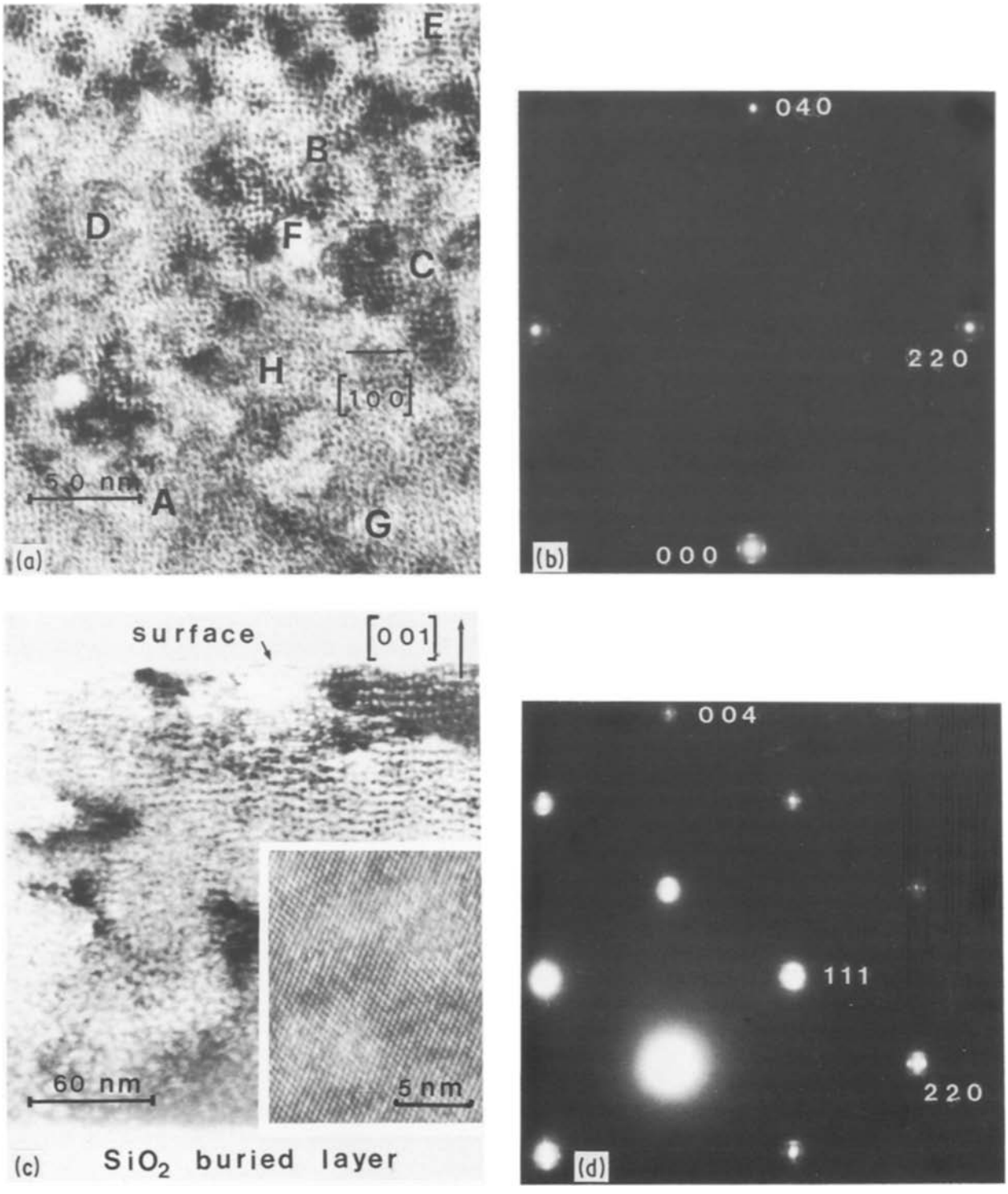

Figure 2 As-implanted specimen. (a) Plane view of the silicon overlayer. The periodic structure of the SiO_2 precipitates along the $\langle 1\,0\,0 \rangle$ directions is evident. (b) Selected-area diffraction from the same area including the origin. The periodicity is about 4.4 ± 0.5 nm. (c) Cross-sectional micrograph from the same specimen section (1 1 0). High resolution TEM observations reveals that these SiO_2 precipitates are free of strain (see inset). (d) Selected-area diffraction from the cross-section. Satellite spots are evident.

they have their ends at the surface and at the $Si-SiO_2$ buried interface.

Stacking faults in bulk silicon are always found to be extrinsic in nature [15–18]. However, in this case we had certain difficulties in determining their nature, due to the complementary contrast of the outer fringes in the bright and dark field (BF, DF) images, for deviation parameter $s = 0$. The discrepancy from the dynamical theory of contrast can be explained from the very low value of the anomalous absorption coefficients of silicon and the relatively thin silicon overlayer, even though the thickness is about three times the extinction distance ξ_g for the 1 1 1 reflection at 100 kV. In order to characterize the observed contrasts, additional observations with $s \neq 0$ diffraction conditions have been made. Fig. 5a is the BF image taken with the 1 1 1 reflection and $s > 0$, while Fig. 5b is the corresponding DF image taken with the $\bar{1}\,\bar{1}\,\bar{1}$ reflection and $s < 0$.

α-fringe profiles have been calculated for the exact

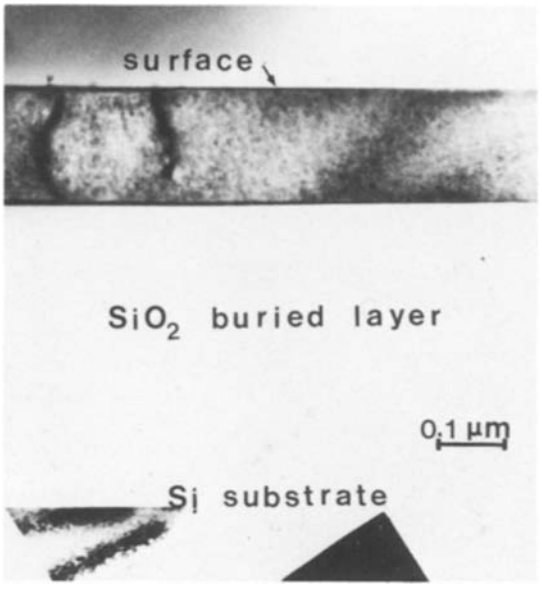

Figure 3 Cross-section of the same specimen as in Fig. 2 after annealing at 1350° C for 6 h. All the SiO_2 precipitates in the silicon overlayer are dissolved with the threading dislocations remaining.

experimental conditions which are given below and correspond to an accelerating voltage of 100 kV:

$$\xi_{111} = 61.8\,\text{nm} \qquad (\xi/\xi')_{111} = 0.013$$

$$w_{111} = 0.2 \qquad w_{\bar{1}\bar{1}\bar{1}} = -0.2$$

where ξ' is the absorption parameter and w the excitation error. The thickness of the specimen is $z_0 = 3.25\,\xi_{111}$. The α-fringe systems of Fig. 6 have the following characteristics:

(i) In the BF and DF images there exists a pseudo-periodicity for the fringe systems of $\xi_{g/2}$.

(ii) In BF, for $z_0 = (3 + 1/4)\xi_g$ in a bright background (BG), the doubled bright fringes have an alternating brighter and less bright intensity, respectively, while the doubled dark fringes are of equal intensity.

(iii) In DF, for $z_0 = (3 + 1/4)\xi_g$ in a bright BG, the doubled dark fringes have an alternating darker and less dark intensity while the doubled bright fringes are of equal intensity.

(iv) BF and DF are complementary even if $s \neq 0$.

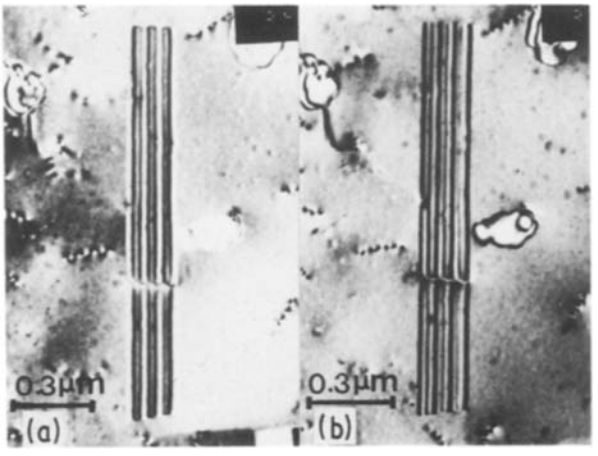

Figure 5 (a) BF image of an SF in a silicon thin film observed in the 1 1 1 reflection, $w = 0.2$. (b) DF image of the same SF observed in $\bar{1}\,\bar{1}\,\bar{1}$, $w = -0.2$.

On the basis of the observed α-fringe contrast of Fig. 5, it was possible to characterize the nature of the SFs by comparing the observed profiles with the calculated ones. Among the computed α-fringe profiles, for different α-values, the best correlation with the observed contrast was obtained with $\alpha = 2\pi/3$ (Fig. 6). Since the operating reflection $\boldsymbol{g} = 1\,1\,1$ and the inclination of the SF have the orientation of Fig. 7, the value of $\alpha = 2\pi/3$ reveals a displacement vector $\boldsymbol{R} = 1/3[1\,1\,\bar{1}]$. Therefore, the SF is extrinsic in character.

The type of the partial dislocations at which the SF terminates was also determined. The lines of these dislocations are almost normal to the trace of the fault. In Fig. 8a, the trace of the fault is along the $[\bar{1}\,1\,0]$ direction and the partials are along the [1 1 2]. These partials are out of contrast only when both the invisibility criteria, $\boldsymbol{g} \cdot \boldsymbol{b} = 0$ and $\boldsymbol{g} \cdot \boldsymbol{b} \times \boldsymbol{u} = 0$, are satisfied. This is evident in Fig. 8b, in which the 2 2 4 reflection operates. The extinction of the dislocations for this reflection implies that the only possible Burgers vector is $(a/3)[\bar{1}\,\bar{1}\,1]$.

A frequently invoked mechanism for the formation of such extrinsic SFs is the consequence of SiO_2 precipitates that are formed during the annealing of the oxygen-rich crystals [19–21]. In the SIMOX struc-

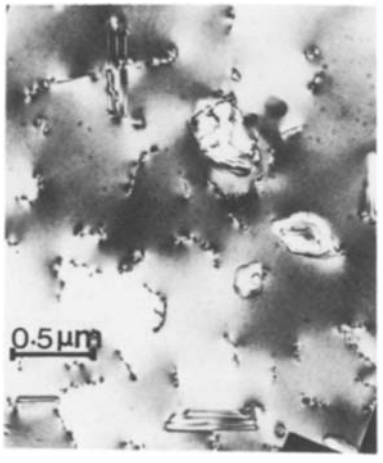

Figure 4 Plane view of the annealed specimen. Stacking faults are evident.

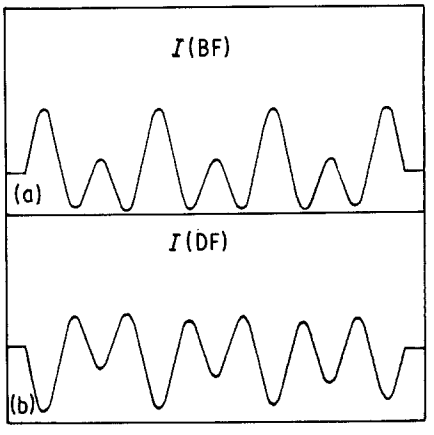

Figure 6 Calculated α-fringe profiles for $\alpha = \pm 120°$; $z_0 = 3.25\,\xi_{111}$, $\xi/\xi' = 0.013$. (a) BF in the 1 1 1 reflection $\alpha = +120°$, $w = 0.2$. (b) DF in the $\bar{1}\,\bar{1}\,\bar{1}$ reflection, $\alpha = -120°$, $w = -0.2$.

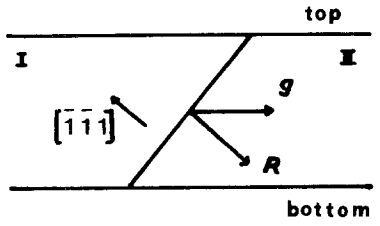

Figure 7 Stacking fault orientation (section 1 1 0).

tures the oxygen concentration is so high that not only an SiO_2 buried layer is formed, but a periodic structure of SiO_2 precipitates in the silicon overlayer is also evident (Fig. 1). This implies the generation of a great number of silicon interstitials. However, in this stage no SFs are formed. In contrast, during the high temperature annealing, where the SiO_2 precipitates are dissolved and the oxygen migrates to the SiO_2 buried layer [22], the SFs appear. This process has to be considered as an SiO_2 redistribution where the generation of silicon interstitials is insignificant.

Due to the fact that the SFs are bounded by two Frank partial dislocations we propose the following mechanism of the dissociation of a perfect dislocation into two partials, according to the reaction [23]

$$\frac{a}{2}\langle 1\,1\,0\rangle \rightarrow \frac{a}{6}\langle 1\,1\,\bar{2}\rangle + \frac{a}{3}\langle 1\,1\,1\rangle \qquad (1)$$

During the annealing, threading dislocations are formed in the silicon overlayer (Fig. 3). These dislocations, according to Hirth and Lothe [24], may belong to the glide or to the "shuffle" set. Most of the glissable dislocations can escape, reducing drastically the dislocation density. Those dislocations which belong to the shuffle set can absorb silicon interstitials and can be dissociated, according to Equation 1, forming the extrinsic SFs. The Shockley partials escape by gliding to the surface, leaving behind the non-glissable Frank type. A schematic representation of the mechanism is illustrated in Fig. 9.

The density of the SFs is heavily dependent upon the implanted dose. For a dose of $2.3 \times 10^{18}\ O^+\ cm^{-2}$ the SF density was $4 \times 10^5 mm^{-3}$; for a dose of $1.8 \times 10^{18} O^+ cm^{-2}$ the SF density was reduced by more than one order of magnitude. Finally, for doses below $1.6 \times 10^{18} O^+ cm^{-2}$ no SFs were observed, even though areas of $6\,mm^2$ of the silicon overlayer were scanned in the electron microscope.

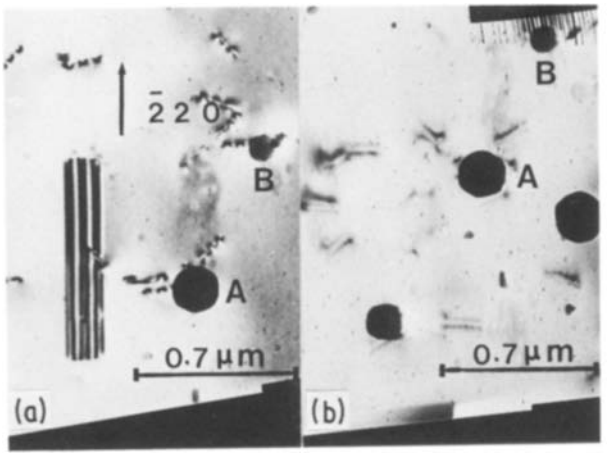

Figure 8 (a) BF micrograph in the 1 1 1 reflection. (b) The same SF after tilting the specimen along the [$\bar{2}$ 2 0] direction for about 55° so that the 2 2 4 reflection operates. The SF as well as the partial dislocations are out of contrast. The black spheres denoted by A and B on the film surface confirm that the observation area is the same.

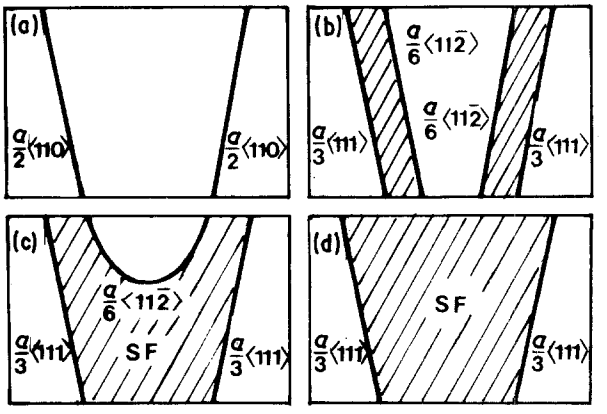

Figure 9 A schematic representation of the mechanism of the dissociation of perfect dislocations into two partials and the formation of the SFs. This formation is possible only if the two perfect dislocations belong to the same plane.

4. Conclusions

1. The SF density in the silicon overlayer is very low, even for high doses of implanted oxygen. This is the reason they have not been observed until now.

2. For the characterization of the SFs, the low value of the anomalous absorption coefficient of silicon and the small thickness of the specimen necessitate experiments with $s > 0$ observation conditions, followed by computer calculation of the α-fringe profiles.

3. The SFs are extrinsic in character, bounded by Frank partial dislocations.

4. The mechanism of the SF formation is not clear. It is most probable that this is related to the dissociation of perfect dislocations.

Further study of the evolution of SFs in SIMOX will help to improve its quality and will lead to a better understanding of the behaviour of the SFs in silicon.

Acknowledgement

For the group at the University of Thessaloniki, this work has been partially supported from the General Secretariat of Research and Technology.

References

1. S. P. MURARKA and G. QUINTANA, *J. Appl. Phys.* **48** (1977) 46.
2. S. M. HU, in "Defects in Semiconductors", 1981 edited by J. Narayan and T. Y. Tan (North-Holland, New York, 1981) p. 333.
3. C. CLAEYS, H. BENDER, G. DECLERCK, J. Van LANDUYT, R. Van OVERSTRAETEN and S. AMELINCKX, *Physica* **116B** (1983) 148.
4. P. L. F. HEMMENT, *Mater. Res. Soc. Symp. Proc.* **33** (1984) 41.
5. P. L. F. HEMMENT, E. MAYDELL-ONDRUSZ, K. G. STEVENS, J. A. KILNER and J. BUTCHER, *Vacuum* **34** (1984) 203.
6. T. HAYASHI, S. MAEYAMA and S. YOSHII, *Jap. J. Appl. Phys.* **19** (1980) 1111.
7. J. STOEMENOS and J. MARGAIL, *Thin Solid Films* **135**

(1986) 115.
8. M. BRUEL, J. MARGAIL, J. STOEMENOS, P. MARTIN and C. JAUSSAUD, *Vacuum* **35** (1985) 589.
9. M. DUPUY, *J. Microsc. Spectrosc. Electr.* **9** (1984) 163.
10. O. W. HOLLAND, T. P. SJOREEN, D. FATHY and J. NARAYAN, *Appl. Phys. Lett.* **45** (1984) 1081.
11. A. H. Van OMMEN, B. H. KOEK and M. P. A. VIEGERS, *ibid.* **49** (1986) 628.
12. J. STOEMENOS, J. MARGAIL, M. DUPUY and C. JAUSSAUD, *Physica Scripta* **35** (1987) 42.
13. C. JAUSSAUD, J. STOEMENOS, J. MARGAIL, M. DUPUY, B. BLANCHARD and M. BRUEL, *Appl. Phys. Lett.* **46** (1985) 1064.
14. J. STOEMENOS, J. MARGAIL, C. JAUSSAUD, M. DUPUY and M. BRUEL, *ibid.* **48** (1986) 1470.
15. G. R. BOOKER and W. J. TUNSTALL, *Phil. Mag.* **13** (1966) 71.
16. J. R. PATEL and A. AUTHIER, *J. Appl. Phys.* **46** (1975) 118.
17. O. L. KRIVANEK and D. M. MAHER, *Appl. Phys. Lett.* **32** (1978) 451.
18. J. R. PATEL, K. A. JACKSON and H. REISS, *J. Appl. Phys.* **48** (1977) 5279.
19. K. WADA, M. INOUE and J. OSAKA, *Mater. Res. Soc. Symp. Proc.* **14** (1983) 125.
20. D. M. MAHER, A. STAUDINGER and J. R. PATEL, *J. Appl. Phys.* **47** (1976) 3813.
21. K. WADA and N. INOUE, *ibid.* **58** (1985) 1183.
22. J. STOEMENOS, C. JAUSSAUD, M. BRUEL and J. MARGAIL, *J. Cryst. Growth* **73** (1985) 546.
23. K. V. RAVI, "Imperfections and Impurities in Semiconductor Silicon" (Wiley, New York, 1981) p. 101.
24. J. P. HIRTH and J. LOTHE, "Theory of Dislocations" (McGraw-Hill, New York, 1968) p. 356.

Received 18 August
and accepted 3 December 1986